

AD_____

AWARD NUMBER: W81XWH-04-1-0034

TITLE: Enhanced Ultrasound Visualization of Brachytherapy Seeds by a Novel Magnetically Induced Motion Imaging Method

PRINCIPAL INVESTIGATOR: Stephen McAleavey, Ph.D.

CONTRACTING ORGANIZATION: University of Rochester
Rochester, New York 14627

REPORT DATE: April 2007

TYPE OF REPORT: Annual

PREPARED FOR: U.S. Army Medical Research and Materiel Command
Fort Detrick, Maryland 21702-5012

DISTRIBUTION STATEMENT: Approved for Public Release;
Distribution Unlimited

The views, opinions and/or findings contained in this report are those of the author(s) and should not be construed as an official Department of the Army position, policy or decision unless so designated by other documentation.

REPORT DOCUMENTATION PAGE				Form Approved OMB No. 0704-0188	
Public reporting burden for this collection of information is estimated to average 1 hour per response, including the time for reviewing instructions, searching existing data sources, gathering and maintaining the data needed, and completing and reviewing this collection of information. Send comments regarding this burden estimate or any other aspect of this collection of information, including suggestions for reducing this burden to Department of Defense, Washington Headquarters Services, Directorate for Information Operations and Reports (0704-0188), 1215 Jefferson Davis Highway, Suite 1204, Arlington, VA 22202-4302. Respondents should be aware that notwithstanding any other provision of law, no person shall be subject to any penalty for failing to comply with a collection of information if it does not display a currently valid OMB control number. PLEASE DO NOT RETURN YOUR FORM TO THE ABOVE ADDRESS.					
1. REPORT DATE 01-04-2007		2. REPORT TYPE Annual		3. DATES COVERED 1 Apr 2006 – 31 Mar 2007	
4. TITLE AND SUBTITLE Enhanced Ultrasound Visualization of Brachytherapy Seeds by a Novel Magnetically Induced Motion Imaging Method				5a. CONTRACT NUMBER	
				5b. GRANT NUMBER W81XWH-04-1-0034	
				5c. PROGRAM ELEMENT NUMBER	
6. AUTHOR(S) Stephen McAleavey, Ph.D. Email: Stephen McAleavey, Ph.D.				5d. PROJECT NUMBER	
				5e. TASK NUMBER	
				5f. WORK UNIT NUMBER	
7. PERFORMING ORGANIZATION NAME(S) AND ADDRESS(ES) University of Rochester Rochester, New York 14627				8. PERFORMING ORGANIZATION REPORT NUMBER	
9. SPONSORING / MONITORING AGENCY NAME(S) AND ADDRESS(ES) U.S. Army Medical Research and Materiel Command Fort Detrick, Maryland 21702-5012				10. SPONSOR/MONITOR'S ACRONYM(S)	
				11. SPONSOR/MONITOR'S REPORT NUMBER(S)	
12. DISTRIBUTION / AVAILABILITY STATEMENT Approved for Public Release; Distribution Unlimited					
13. SUPPLEMENTARY NOTES Original contains colored plates: ALL DTIC reproductions will be in black and white.					
14. ABSTRACT We report our progress in developing Magnetically Induced Motion Imaging (MIMI) for unambiguous identification and localization brachytherapy seeds in ultrasound images. In this period we have used finite-element models to determine a torque maximizing seed core shape to generate the greatest possible seed vibration for a given core volume. We present two new signal-processing methods. The first is a compounding method for suppression of "comet-tail" artifacts in segmented seed images. The second is a method for joining ends of seeds in segmented seed images based on the phase of the detected vibration signal. Both methods are demonstrated in vitro using a commercial ultrasound scanner and tissue-mimicking phantoms.					
15. SUBJECT TERMS Brachytherapy Seeds					
16. SECURITY CLASSIFICATION OF:			17. LIMITATION OF ABSTRACT	18. NUMBER OF PAGES	19a. NAME OF RESPONSIBLE PERSON
a. REPORT	b. ABSTRACT	c. THIS PAGE			USAMRMC
U	U	U	UU	15	19b. TELEPHONE NUMBER (include area code)

Table of Contents

	<u>Page</u>
Introduction.....	4
Body.....	4
Key Research Accomplishments.....	6
Reportable Outcomes.....	7
Conclusion.....	7
References.....	7
Appendices.....	8

Introduction

We have devised a method called Magnetically Induced Motion Imaging (MIMI) for identifying brachytherapy seeds in ultrasound images. Ultrasound guided brachytherapy [Holm1983, Nag1997] is a common treatment for prostate cancer. The overall goal of this project is the unambiguous identification and accurate localization of brachytherapy seeds with ultrasound. Accurate determination of seed location is critical in delivering the correct dose distribution to the prostate. Automatic seed segmentation and real-time dose planning are enabled by this technique. Furthermore, the technique enables ultrasound to replace CT for post-implant evaluation, by providing a mechanism by which implanted seeds may be reliably identified by ultrasound. The proposed research will investigate and optimize the materials, instrumentation and algorithms for MIMI, to develop simulation, analytic and phantom methods to explore the relevant phenomena, and to conduct clinically realistic evaluations of the method.

Body

This report documents activities related to this grant for the period of April 1 2006 to March 30 2005. The grant was originally awarded to the PI April 1 2004 at Duke University. The work was suspended the following month when the PI transferred to the University of Rochester. Work resumed at Rochester June 2005. The PI applied for and was granted a no-cost extension to cover the interruption in work so all tasks may be completed.

The Statement of Work identifies the following tasks:

Task 1. Modeling of seed electromechanics (Months 1-18)

- A) Propose magnetic core geometry
- B) Develop finite-element model of magnetic seed core for electromagnetic simulation
- C) Solve for seed forces as a function of field strength, orientation and gradient
- D) Iteratively modify core design to maximize induced force given a constant-volume constraint

Task 2. Modeling of seed-tissue mechanics (Months 6-24)

- A) Develop finite-element mesh of seed and tissue
- B) Solve for steady-state vibration amplitude over 50-500Hz band
- C) Calculate vibration amplitude of seed vs. frequency
- D) Find iso-amplitude contours within tissue as a function of vibration frequency

Task 3. Seed detection algorithm development (Months 12-36)

- A) Simulate ultrasound RF echoes from seed and tissue vibrating as determined in Task 2 for varying seed-beam angle
- B) Evaluate motion detection and clutter suppression methods
- C) Determine vibration frequency which provides maximum spatial resolution

Task 4. In-vitro implementation (12-36)

- A) Fabricate or procure model seeds based on core design developed in Task 1
- B) Procure prostate phantom
- C) Implant seeds and clutter targets in prostate phantom
- D) Capture RF echo data and generate seed images using the algorithm of Task 3
- E) Implant seeds in excised animal tissue samples and image using the algorithm of Task 3

Here we describe our progress with regard to these tasks since the last annual report.

Task 1: Seed electromechanical force modeling

Simulation of seed electromagnetic forces continued during the period of this report using FEMLAB (Comsol AB) finite-element package and the Maxwell Stress Tensor method [Wangness1986]. Our goal is to find the magnetic core shape that maximizes this torque subject to constraints on volume, maximum length, and maximum width imposed by the shape of a standard brachytherapy seed. In the previous report period we had developed 3D finite-element models for two seed magnetic-core geometries, an ellipsoid and a rod capped by two semi-hemispheres. These initial models were allowed straightforward comparison to analytical torque models [Jones1995].

In the current report period we extended these models to allow simulation of and calculation of torques on more complex shapes. In carrying out this work we took advantage of an electric-magnetic duality. The problem of estimating torque on a linearly magnetizable due to an applied magnetic field is equivalent to the problem of estimating torque due to an electric field on a dielectric particle. Just as the magnetic brachytherapy seed cores experience a torque when placed in a magnetic field due to induced magnetization, a non-polarized dielectric particle of isotropic material suspended in an electrostatic field experiences a torque by induced polarization due to shape anisotropy.

We have employed two new finite element models to find a torque-maximizing core shape. In our first model, particles were modeled as a pair of symmetric frusta (what is left of a cone after the with the top part is cut off parallel to the base) joined at their faces to form tapered, rod-like shapes. The radii of the rod ends were equal and the radius at the particle's waist adjusted to maintain constant volume. The torque-maximizing shape is strongly dependent ϵ_r , the particle's relative permittivity, low values favoring mass concentration near the waist of the particle and high values favoring concentration of mass near the ends. A more detailed model was created as a stack of nine frusta subject to the same symmetry and constant-volume constraints. For high relative permittivity material ($\epsilon_r = 4000$), a shape with mass concentrated at the ends of the particle, gives the highest torque.

The details of the modeling are presented in the attached paper "Shape optimization of elongated particles for maximum electrical torque," presented at the 2007 Electrostatic conference of the Institute of Physics. The key result of this work is that for highly magnetizable materials, as would be used for the proposed brachytherapy cores, there is a slight advantage in torque to be gained by distributing the core material towards the end of the seed. The maximum improvement compared to a simple cylinder, on the order of 10%, may not be sufficient in practice to justify the cost of shaping the core. A second interesting result, albeit of limited utility in the brachytherapy seed problem, is that the torque maximizing shape is a function of the magnetic permeability (electric permittivity) of the seed core.

Task 2: Modeling of seed-tissue mechanics

No new simulations of seed-tissue mechanics were carried out during the period of this report.

Tasks 3 and 4: Seed detection algorithm development and in-vitro implementation

Our recent developments in seed detection algorithms and in-vitro implementation of these methods were presented at the 2006 IEEE Ultrasonics Symposium in our paper "Magnetically Vibrated Brachytherapy Seeds: Ferromagnetic Core Models and Image Reconstruction Methods," attached. The principle research results are the development of a compounding technique to reduce "comet-tail" ringdown artifacts in seed images, and a directional blurring method to link seeds together. The data acquisition methods and experimental procedures are similar to those detailed in the previous annual report, while the details of these new methods are presented in the IEEE paper. A summary of these methods is presented here.

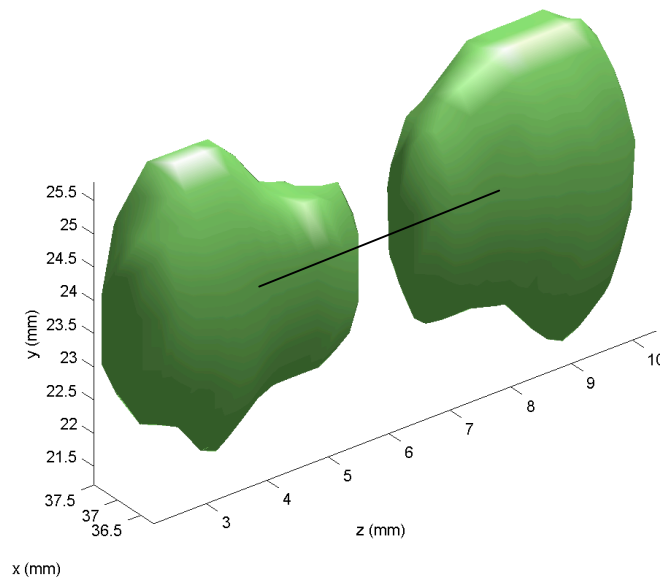


Figure 1. Isosurface volume rendering of seed and tissue vibration from Color Doppler data. The seed location is approximately denoted by the line. The transducer scan plane is the x-z plane. The volume reconstruction was performed by stepping along the y axis in 1mm steps. The lower out-of-plane resolution results in the greater apparent size in the y direction.

As shown in Figure 1 here, and in Figure 4 of the IEEE paper, a seed rocking about its center naturally has the greatest vibration amplitude at its ends. An image of vibration amplitude thresholded to a particular value will result in a “dumbbell” shape seed image. Ideally, the detected shape would completely enclose the seed and approximate its shape. The directional blurring methods described uses the phase of the vibration signal to determine the orientation of the seed and link opposite seed ends, resulting in a seed image which encloses the seed and more accurately describes its shape and orientation.

A second imaging artifact is the “ring-down” or “comet-tail” artifact due to ultrasound reverberation within the seed. The result of this reverberation is a tail in the image that proceeds away from the seed in the direction of the ultrasound beam. This tail complicates image segmentation and interpretation and could result in a mistaken estimate of seed orientation.

The compounding technique described in the paper combines seed images obtained from multiple angles to suppress the ring down artifact. This method uses the principle that, while the tail will change position as the ultrasound beam is steered, the seed itself remains fixed. We acquire seed images at two different beam angles and threshold to create a pair of binary images. A final seed image is created by calculating the pixelwise logical AND of each image. The comet tails, with their different position in each image, are suppressed, while the seed itself is unaffected. This method and result is described in section IIIC of the IEEE paper and illustrated in figures 4-7.

Key research accomplishments in this period:

- Finite-element model of electromagnetic force on two seed geometries
- Demonstration of sensitivity of torque to seed geometry
- Estimation of a torque-maximizing seed core shape
- Image processing method for joining ends of seeds in segmented images
- Demonstration of method for suppressing ring-down artifact

Reportable Outcomes:

Publications:

1. Stephen A. McAleavey, Scott White, Manoj Menon, Magnetically Vibrated Brachytherapy Seeds: Ferromagnetic Core Models and Image Reconstruction Methods,” *Proceedings of the IEEE Ultrasonics Symposium*, pp1103-1106, 2006
2. Stephen A. McAleavey, Thomas B. Jones, Nicholas G. Green, “Shape Optimization of Elongated Particles for Maximum Electrical Torque,” *Proceedings of Electrostatics 2007*

Conclusions:

This report has described the work performed from April 2006 to March 2007. Significant progress was made in Tasks 1, 3 and 4. The important simulation result is the determination of a torque-maximizing magnetic core shape. We have developed and demonstrated in vitro a technique for suppression of ring-down artifacts in segmented seed images. We have also demonstrated a method for elimination of the “dumbbell” artifact, allowing accurate segmentation of a seed as a single unit, rather than as a pair of seed ends.

References:

- [Comsol2004] *Electromagnetics Module User's Guide*, Comsol AB, 2004
- [Holm1983] H.H. Holm, N. Juul, J.F. Pedersen, H. Hansen, I. Stroyer, “Transperineal (125)Iodine Seed Implantation in Prostatic Cancer Guided by Transrectal Ultrasonography”, *Journal of Urology* v.130, pp.283-286, August 1983
- [Jones1995] T. B. Jones, *Electromechanics of Particles*, Cambridge, 1995
- [Nag1997] S. Nag, V. Pak, J. Blasko, P.D. Grimm, “Brachytherapy for Prostate Cancer” in *Principles and Practice of Brachytherapy*, Futura, 1997
- [Surry2004] K.J.M. Surry, H.J.B. Austin, A. Fenster, T.M. Peters, “Poly(vinyl alcohol) cryogel phantoms for use in ultrasound and MR imaging,” *Physics in Medicine and Biology* 49, pp. 5529-46, 2004
- [Wangsness1986] R.K. Wangsness, *Electromagnetic Fields*, John Wiley and Sons, 1986

Shape optimization of elongated particles for maximum electrical torque

S A McAleavey^{1*}, T B Jones¹, and N Green²

¹University of Rochester (USA) and ²University of Southampton (UK)

*Correspondance: stephenm@bme.rochester.edu

Abstract: A non-polarized particle of isotropic material suspended in an electrostatic field experiences a torque by induced polarization due to shape anisotropy. This torque is a strong function of shape and has a lower bound of zero in the limit of a sphere. Our goal has been to find the particle shape that maximizes this torque subject to constraints on volume, maximum length, and maximum width. In particular, the particle must fit within a cylinder of length to width ratio 11:1, and must occupy no more than 1/3 of the cylinder volume. We have employed a finite-element approach to search for this shape. In our first model, particles were modelled as a pair of symmetric frusta joined at their faces to form tapered, rod-like shapes. The radii of the rod ends were equal and the radius at the particle's waist adjusted to maintain constant volume. The torque-maximizing shape is strongly dependent ϵ_r , the particle's relative permittivity, low values favouring mass concentration near the waist of the particle and high values favouring concentration of mass near the ends. A more detailed model was created as a stack of nine frusta subject to the same symmetry and constant-volume constraints. For high relative permittivity material ($\epsilon_r = 4000$), a shape with mass concentrated at the ends of the particle, gives the highest torque.

1. Introduction

It is well known that a non-polarized particle of isotropic material in an electrostatic field experiences a torque due to induced polarization [1,2]. This torque is determined by the shape of the particle for a given field strength, particle volume, and permittivity. We have investigated the dependence of torque on shape and found that, when the geometry of the particle is constrained, the torque-maximizing shape is dependent on the permittivity of the particle.

The motivation for this work is the development of a method for imaging prostate brachytherapy seeds [3-4]. In this application a brachytherapy seed is a cylinder of length 4.5mm and diameter 0.8mm. The seeds contain a radioisotope and are implanted in the prostate as a cancer therapy. If made to vibrate in situ these seeds can be identified by Doppler ultrasound imaging methods. Vibration is induced by loading the seeds with a ferromagnetic core and subjecting the implanted seeds to an oscillating magnetic field. A design goal is to determine the core shape that produces the maximum vibration amplitude for a given volume of core material constrained to fit within a seed. When a linear magnetic model is used ($B = \mu_r \mu_0 H$) the electrostatic and magnetostatic problems are equivalent.

2. Theory

A non-polarized isotropic particle of permittivity ϵ_2 and volume V in a fluid of permittivity ϵ_1 experiences a torque when an electric field E is applied. The torque is given by [1]

$$T = -VE^2 \frac{(\epsilon_2 - \epsilon_1)^2 (L_{\parallel} - L_{\perp})}{\epsilon_1 \left(1 + \frac{\epsilon_2 - \epsilon_1}{\epsilon_1} L_{\parallel}\right) \left(1 + \frac{\epsilon_2 - \epsilon_1}{\epsilon_1} L_{\perp}\right)} c_x c_z$$

where L_{\perp} and L_{\parallel} are functions of particle shape. The equivalent expression for an isotropic linear magnetic particle with permeability $\mu_r \mu_0$ is $T = -V\mu_0 H_0^2 \frac{\chi^2 (L_{\parallel} - L_{\perp})}{(1 + \chi L_{\parallel})(1 + \chi L_{\perp})} c_x c_z$ where

$\chi = \mu_r - 1$. The two expressions are equivalent when $\epsilon_2 = \mu_r \mu_0$ and $\epsilon_1 = \mu_0$. Torque may be calculated conveniently for the case of spheroids where analytical solutions for L_{\perp} and L_{\parallel} are known [3]. For a prolate spheroid with major to minor axis ratio $r = a/b$, the spheroid eccentricity is defined as $e = \sqrt{1 - 1/r^2}$, $L_{\parallel} = \frac{1}{2r^2 e^2} \left(\ln \left(\frac{1+e}{1-e} \right) - 2e \right)$ and $L_{\perp} = (1 - L_{\parallel})/2$. In the limit as r tends to infinity $L_{\parallel} \rightarrow 0$ and $L_{\perp} \rightarrow 1/2$ so that the limiting value of T is $VE^2 (\epsilon_2 - \epsilon_1)^2 / (\epsilon_2 + \epsilon_1)$ or $V\mu_0 H_0^2 \chi^2 / (2 + \chi)$ for the magnetic case.

The above expressions may be solved to calculate torque as a function of r normalized by the limiting torque value given above for a fixed V . Figure 1a is a plot of this solution for several values of relative permittivity $\epsilon_r = \epsilon_2/\epsilon_1$. For all values of ϵ_r the torque increases with particle elongation (increasing r). The increase in torque with r is most rapid for small values of ϵ_r , implying particles with a high relative permittivity require a greater elongation to reach a fixed fraction of the maximum torque. This is depicted in figure 1b, a plot of the value of r required to reach 90% of the limiting torque value as a function of ϵ_r . Finally, figure 1c shows that the dependence of normalized torque as a function of V for a fixed length spheroid varies with ϵ_r . As expected, for a fixed length ellipsoid torque does not monotonically increase with V , as increasing volume transforms the spheroid into a sphere. Interestingly, the torque maximizing volume for a given major axis length depends on ϵ_r . Peak torque is achieved with a smaller volume for larger values of ϵ_r . Smaller values of ϵ_r favor a larger volume. These results suggested that the core shape sought for the brachytherapy seed will be dependent on μ_r , and that a torque maximizing particle shape in general will be dependent on ϵ_r .

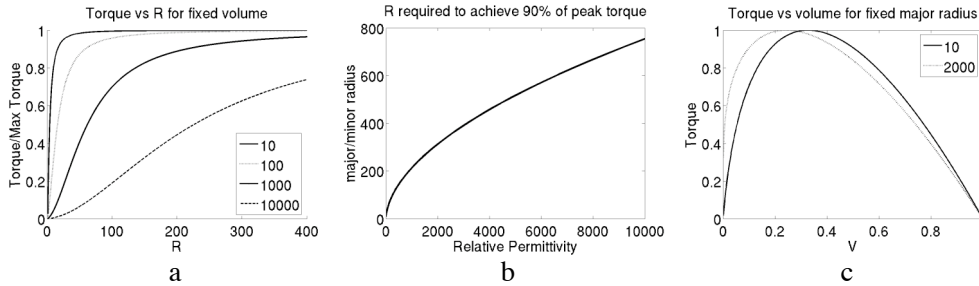


Figure 1. (a) Torque as a percentage of maximum value increases more slowly with particle length for a fixed volume as permittivity increase, as shown here for the indicated permittivities. (b) This same relationship shown as a function of permittivity. (c) For a spheroid of fixed major axis length, the volume, and hence shape, required to maximize torque depends on particle permittivity.

3. Methods

Torques on non-spheroidal particles were calculated using the Comsol Multiphysics finite element package (Comsol, Inc., Burlington, MA). Two models were considered. The first treats the particle as a stack of two frusta (truncated cones), as illustrated in figure 2a. The particles simulated had a fixed length 0.5cm and fixed volume. The ratio of end and center radii was varied to take the particles through a range of shapes from “bowtie” to “diamond,” thus there was only one degree of geometrical freedom, $R=r_{\text{end}}/r_{\text{center}}$. The torque for each shape was calculated for ϵ_r values of 3, 30, 300, 3000. The torque was calculated by integrating the product of Maxwell Stress Tensor times the lever arm over the surface of the particle. Torques for the two-frusta particle were calculated for a range of R of 0.6 to 3.7.

A model composed of a stack of 9 frusta was constructed to search for a torque-maximizing shape with more degrees of freedom. The model had a fixed length of 0.5 cm and volume of $0.022\pi \text{ cm}^3$. As in the two-frusta model, lateral symmetry was imposed on the seed. Combined with the fixed volume constraint this model had two degrees of freedom, illustrated in figure 2b. Torques on this model were calculated for $r1$ and $r2$ ranging from 0.15 to 0.25, with $r3$ calculated to maintain constant volume for particular $r1$ and $r2$. In addition a guided optimization was sought using Matlab’s **fmincon** function, which uses a sequential quadratic programming method to search for an optimum. A five-element model vector \mathbf{y} described the seed radii at as many points over half its length, lateral symmetry and constant volume again being imposed. Calls to the Comsol solver returned torque values for a requested \mathbf{y} , allowing the five-dimensional space to be searched efficiently.

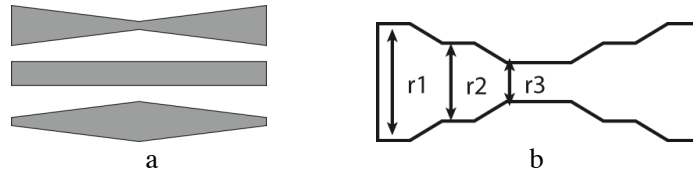


Figure 2. (a) Two and (b) nine frusta particle models. Constant volume is maintained for all.

4. Results

Figure 3a presents the calculated torque for the two-frusta normalized to the peak torque as a function of R for ϵ_r values of 3, 30, 300, and 3000. The results show the same trend suggested by the spheroid calculations. Particles with a low relative permittivity maximize their torque when their mass is concentrated toward their center. The mass of the torque-maximizing shape shifts towards the ends of the particle with increasing values of ϵ_r .

Figure 3b presents a contour plot of seed torques calculated for the model of figure 2b at the indicated values of $r1$ and $r2$, with $r3$ determined by the constant volume constraint, normalized to the maximum value calculated. The model had a relative permittivity of 3000. A cylinder of constant radius 0.21 generated a torque of 79% as great as the peak value, obtained with radii $r1=0.220$, $r2=0.314$, $r3=0.194$. This result again shows torque is increased with mass concentrated towards the seed ends.

The constrained minimization search performed poorly, due to noise in the simulation arising from mesh changes with seed shape and numerical error. Future work on shapes with a greater number of degrees of freedom will require less noise-sensitive search methods.

5. Discussion

Both the analytical spheroid calculations and the finite element results indicate that the torque-maximizing shape varies as a function of permittivity. The total spheroid volume required for a fixed major axis length particle to achieve maximum torque for a given material permittivity is not constant as shown in figure 1c. The finite element model showed that the torque maximizing

two-frusta shape varied as a function of permeability/permittivity. Low values of ϵ_r favor a mass concentration near the particle waist, while high ϵ_r results in mass concentration at ends. The finite element model for the particle of figure 2b also favored an end-weighted shape consistent with its relatively high permittivity.

The torque optimization problem is challenging for particles whose shape has many degrees of freedom. The constrained search method was found to be susceptible to “noise” in the simulation due to variations in torque calculated for a given shape with different meshes. The variation in torque was on the order of 1-2% for different randomly generated meshes. This variation was often enough to confound the search algorithm. Search methods with better noise immunity, such as simulated annealing, may lead to better results.

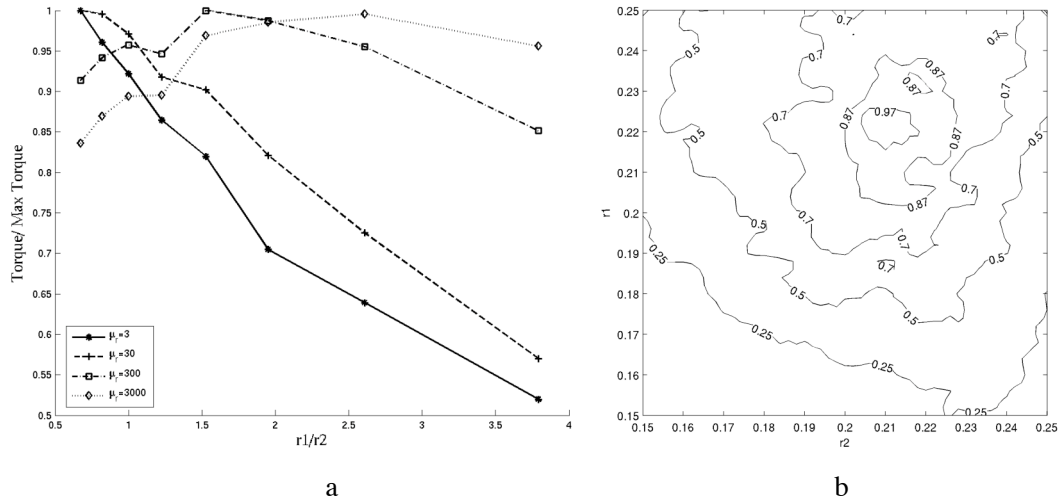


Figure 3. (a) Plots of the calculated torque for the particles of figure 2b for the indicated values of relative permittivity (3-3000) as a function of R . The peak torque moves to higher values of R as ϵ_r increases. (b) Contour plot of torques calculated for the particle of figure 2b for the radii r_1 and r_2 shown on the axes.

6. Conclusion

Though a combination of finite element methods and analytical solutions we have demonstrated that the particle shape that maximizes electrical torque is dependent on the ratio of particle permittivity to that of its environment ϵ_r . For a fixed particle length, particles with small values of ϵ_r experience maximum torque when their mass is concentrated towards the center, while particles with a larger value of ϵ_r realize their greatest torque with their mass distributed towards the ends of the particle. The results suggest that a magnetic core for the brachytherapy seed application described should be end-weighted.

References

- [1] Jones T B 1995 *Electromechanics of Particles* (New York: Cambridge)
- [2] Stratton J A 1941 *Electromagnetic Theory* (New York: McGraw-Hill)
- [3] McAleavey S A, Rubens D J and Parker K J 2003 Doppler ultrasound imaging of magnetically vibrated brachytherapy seeds *IEEE Trans Biomed Eng* **50** 252-5
- [4] McAleavey S A 2002 Doppler technique for the detection and localization of modified brachytherapy seeds” *Proc of SPIE* **4687** 190-198

Magnetically Vibrated Brachytherapy Seeds:

Ferromagnetic Core Models and Image Reconstruction Methods

Stephen A. McAleavey, Scott White, Manoj Menon

Department of Biomedical Engineering

University of Rochester

Rochester, NY., USA

stephenm@bme.rochester.edu

Abstract—Magnetically Induced Motion Imaging (MIMI) uses an oscillating magnetic field and ultrasonic motion-tracking techniques to vibrate and identify brachytherapy seeds in situ. The efficacy of the technique relies on the ability to generate and detect seed vibration, and distinguish this vibration signal from other motion sources. The vibration of the seed depends on the torque generated by a ferromagnetic core in the seed. A design goal is to maximize the torque for the limited amount of core material that can be placed within a seed. We have developed 3D finite-element models for two seed core geometries, an ellipsoid and a rod capped by two semi-hemispheres. Both seed cores have identical volumes ($7.4 \times 10^{-10} \text{ m}^3$), length (4mm), and permeability ($\mu_r=4000$). Calculation by the Maxwell Stress Tensor method yields a torque for the rod 1.4 times that of the ellipsoidal core, demonstrating the substantial sensitivity of torque on core geometry.

The oscillating seeds act as dipole shear wave sources, with maximum vibration amplitude at the ends of the seed and a vibration minimum at the center of length. This gives rise to a characteristic vibration amplitude distribution in the surrounding tissue, with two lobes per seed. By taking advantage of the opposing phase of the seed ends, we demonstrate a method that links these lobes. A compounding technique for suppressing ring-down artifact is demonstrated. These methods are demonstrated on RF data acquired from seeds in beef muscle tissue. 3D vibration isosurface maps of seed vibration amplitude are presented and found to be in good agreement with previously reported simulations.

I. INTRODUCTION

We have previously reported a technique for imaging brachytherapy seeds called Magnetically Induced Motion Imaging (MIMI) [1,2]. Modified brachytherapy seeds containing a ferromagnetic core are made to oscillate about their center due to the time-varying torque induced on the cores. The vibration amplitude of the seed and surrounding tissue is on the order of 1 micron and is detected by ultrasonic motion tracking methods.

II. SEED CORE TORQUE

In the modified seeds the limited volume of the seed must be shared between the therapeutic radioisotope and the ferromagnetic core. The finite volume available to the core should be used as efficiently as possible to maximize the

torque on the seed, and thus its vibration, for a given magnetic field to improve sensitivity. The torque T on a ferromagnetic particle of isotropic permeability μ_r and volume V in a magnetic field of strength H_0 is a function of

its shape [3], $T = -V\mu_0 H_0^2 \frac{\chi^2(L_{\parallel} - L_{\perp})}{(1 + \chi L_{\parallel})(1 + \chi L_{\perp})} c_x c_z$, where

L_{\perp} and L_{\parallel} are shape functions and $\chi = \mu_r - 1$ the magnetic susceptibility. Torque may be calculated conveniently for the case of spheroids where analytical solutions for L_{\perp} and L_{\parallel} are known [3]. For a prolate spheroid with major to minor axis ratio $r = a/b$, the spheroid eccentricity is defined as $e = \sqrt{1 - 1/r^2}$, $L_{\parallel} = \frac{1}{2r^2 e^2} \left(\ln \left(\frac{1+e}{1-e} \right) - 2e \right)$ and

$L_{\perp} = (1 - L_{\parallel})/2$. Torque versus r for a unit volume prolate spheroid in a unit field H is plotted Figure 1. In the limit as r tends to infinity $L_{\parallel} \rightarrow 0$ and $L_{\perp} \rightarrow 1/2$ so that the limiting value of T is $V\mu_0 H_0^2 \chi^2 / (2 + \chi)$. For a fixed length ellipsoid torque does not monotonically increase with r , as shown in Figure 2. For a fixed a , V increases as r decreases. For the dimensions of a brachytherapy seed, using the largest ellipsoid that fits in the seed maximizes torque.

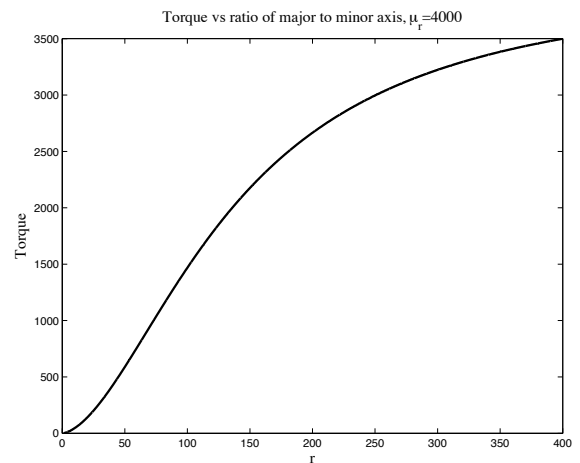


Figure 1. Torque increases monotonically for a constant volume ellipsoid as the ellipsoid transforms from spherical to highly eccentric.

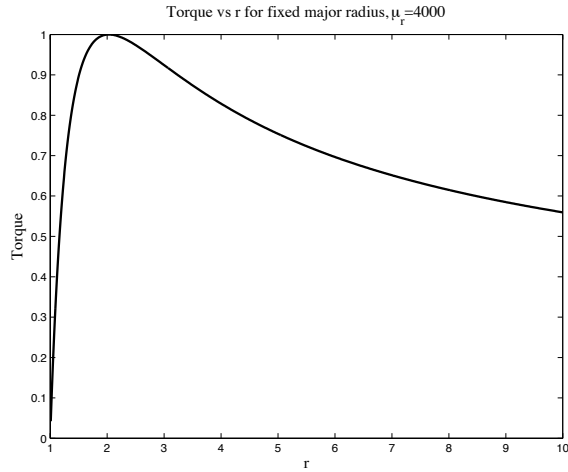


Figure 2. For a fixed length ellipsoid, the combination of varying volume and eccentricity give rise to a non-monotonic variation in torque. Typical brachytherapy seed dimensions imply that r can be no less than 10. Therefore the widest (largest b) ellipsoid that can be fit in the seed will maximize torque.

Clearly torque is a strong function of shape. To compute torque on non-spheroids a finite element model constructed using Comsol Multiphysics finite element software (Comsol, Inc. Burlington, MA). Spheroids and cylinders of identical volume ($7.4 \times 10^{-10} \text{ m}^3$, one third the volume of a seed) were modeled [4]. These shapes were selected to allow straightforward comparison to analytical torque models. The flux B in the core material was modeled as linearly dependent on H , $B = \mu_0 \mu_r H$, with an isotropic relative permeability $\mu_r = 4000$. The torque exerted on the seed was calculated by the Maxwell Stress Tensor method [5]. Torque was calculated at a field value of $H = 1 \text{ A/m}$ and scales as H^2 . The finite-element calculated value for ellipsoid torque was $1.61 \times 10^{-14} \text{ Nm}$, in good agreement with the analytical value of $1.53 \times 10^{-14} \text{ Nm}$. The torque on the cylinder was calculated as $2.28 \times 10^{-14} \text{ Nm}$, ~ 1.4 times the torque of the ellipsoidal core.

III. SEED DETECTION

A. Experimental Method

Ferromagnetic seed cores were cut from 0.5mm diameter piano wire to a length of 5 mm. The seed cores were embedded in beef muscle tissue obtained from a local butcher. The seeds were induced to vibrate with a 13cm diameter coil of 200 turns of 18-gauge wire. The magnetic field at the center of the coil is given by $NI/2r$, where N is the number of turns, I the current, and r the coil radius. The maximum field value at the coil center was $\sim 6,200 \text{ A/m}$ at 50Hz. The measured resistance and inductance were 3ohms and 7.4mH. During scanning the axis of the coil was set at a 45° angle to the long axis of the seeds. The coil was driven by a 200W audio amplifier connected to a function generator at frequencies of 50 to 300Hz. RF echo data from the vibrating seeds and tissue were acquired using a Siemens Antares scanner and the Axis Direct Research Interface

with a VF10-5 linear array. The PRF of the Doppler sequence used was chosen to be 2.5-3 times the seed vibration frequency, within the available scanner settings. Three-dimensional RF data sets were acquired by translating the transducer in the elevational direction in 0.5mm increments.

Displacements were tracked using the 1D autocorrelation method of Kasai [6]. In contrast to standard Doppler tracking where phase shifts are averaged at a given depth over the Doppler ensemble, here phase shifts averaged in the axial direction over a distance of 1mm. Low frequency environmental vibration was removed by fitting and subtracting a linear component of displacement from the data. Vibration was quantified by calculating the RMS value of the remaining motion signal.

Figure 3a shows the measured coil current for a 500mV peak-peak amplifier current. The amplifier has a constant voltage gain, while torque is proportional to the square of current. Constant torque was maintained by adjusting the amplifier drive voltage to maintain constant current. Figure 3b shows vibration measured at the seed tip at 100 and 300 Hz with constant current drive. Vibration amplitude is on the order of $0.1 \mu\text{m}$ and roughly equal at each frequency.

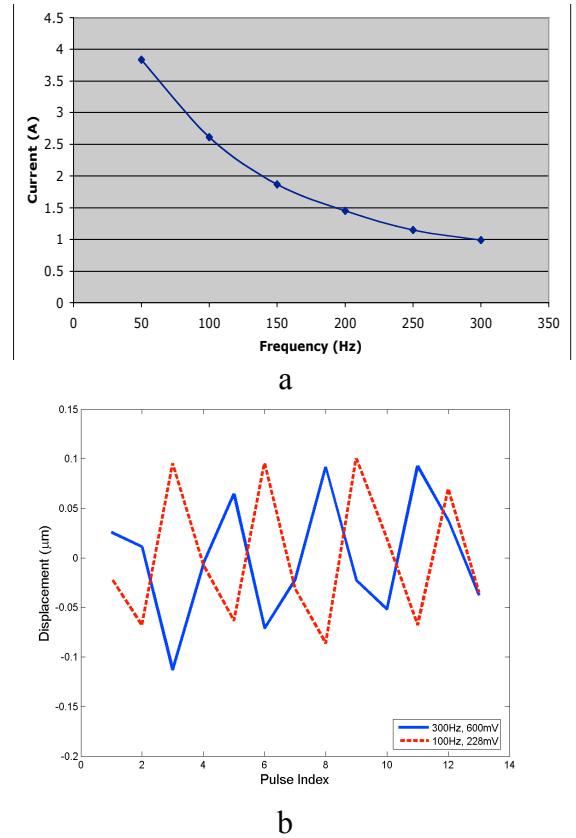


Figure 3. (a) Measured current in coil as a function of frequency for 500mVpp amplifier drive. As torque varies with the square of current, the vibration amplitude at 50Hz is $\sim 16\times$ larger than at 300Hz for constant input. (b) Measured seed tip displacements in beef tissue at 100 and 300Hz. Note the horizontal axis is pulse index, not time. The PRFs used were 610Hz and 1953Hz for the 100 and 300Hz signals. The input voltage was scaled to provide equal coil currents at both frequencies.

B. Synchronous detection and directional blurring

Synchronous detection of seed vibration was achieved by selecting the vibration frequency such that an integer number of cycles occur between Doppler ensembles. The displacement estimates $u(x,n)$ were then detected according to the relation $p(\vec{x}) = \sum_{n \in \text{ensemble}} u(\vec{x},n) \cos(2\omega_0 n / PRF)$, where

ω_0 is the coil drive frequency, the vibration frequency being twice that due to the squared dependence of torque on current. The sign of p indicates whether the motion phase is 0° or 180° . The positive and negative components of p may be blurred in opposing directions to link the seed ends together, as illustrated in figure 5, allowing the seed to be segmented as a single object. The directionally blurred image was formed by creating two sub-images, $p_+(\vec{x}) = p(\vec{x})(p(\vec{x}) > 0)$ and $p_-(\vec{x}) = -p(\vec{x})(p(\vec{x}) \leq 0)$, where the inequalities at a given x evaluate to 1 if true and 0 if false. These sub-images were convolved with filters possessing rightward and leftward bias (here a string of eight 1's followed by eight 0's and its reflection) and the results summed. In this way p_+ experiences a rightward blur while p_- experiences a leftward blur.

C. Ring down suppression:

Vibration amplitude isosurfaces generated from the 3D RF data often shows a ring-down artifact in the form of a "tail" distal to the seed, as in figure 6a. The ring-down tail is also evident in the displacement maps of figures 4 and 5. The tail appears in the image to proceed away from the seed in the direction of beam propagation, as acoustic energy continues to echo back from the reverberant seed. Changing the look direction by steering the ultrasound beam will cause the apparent location of the tail to change relative to the seed.

This tail may be eliminated by scanning from two or more look directions using the typical beam-steering control found in Color Doppler systems. The process is illustrated schematically in figure 7. Estimation of vibration amplitude is carried out on each data set independently. The data sets are thresholded to the isosurface value, and the product of the segmented volumes taken. As the location of the tail varies with steering angle while the seed location remains constant, the seeds are retained while the ring-down tails are suppressed.

This technique is demonstrated in Figures 6. Two parallel seeds embedded in beef tissue were scanned. Here the z axis represents the axial (beam) direction, the x axis the lateral image dimension, and y the out-of-plane dimension. The transducer was mounted on a three-axis positioner and moved in 0.5mm steps, while the seed was vibrated with the coil described above and an amplifier input of 600mVpp at 200Hz. The alignment of the seeds and transducer was selected to emphasize the ringdown artifact in the left-hand seed. Figure 6a illustrates the vibration amplitude isosurfaces generated for a straight-ahead (0° beam steering). The tails are clearly visible. Figure 8 was formed by collecting two echo data sets with beams steered at $\pm 15^\circ$. Each displacement data set was segmented at the same isosurface value as figure 6a. The segmented volumes were

then multiplied on a voxel-by-voxel basis to arrive at the isosurface map shown in figure 6b.

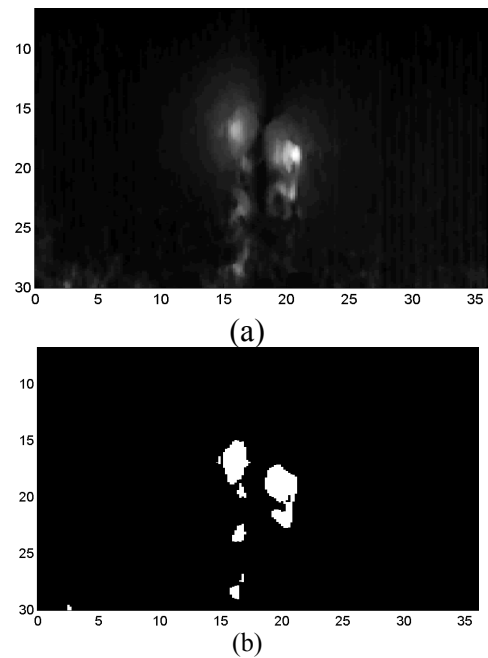


Figure 4. (a). Displacement map of estimated tissue displacement of seed in beef muscle. White represents $0.5\mu\text{m}$ RMS vibration amplitude, black $0\mu\text{m}$. Note the dipole shape of the vibration field. (b) The vibration field thresholded at $0.3\mu\text{m}$ RMS.

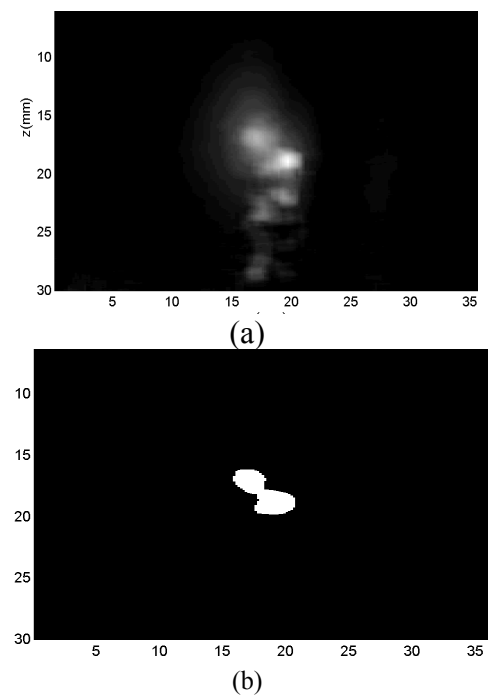


Figure 5. (a). Displacement map of estimated tissue displacement of seed in beef muscle following phase-sensitive blurring. White represents $0.5\mu\text{m}$ RMS vibration amplitude, black $0\mu\text{m}$. Note the dipole shape of the vibration field. (b) The vibration field thresholded at $0.3\mu\text{m}$ RMS.

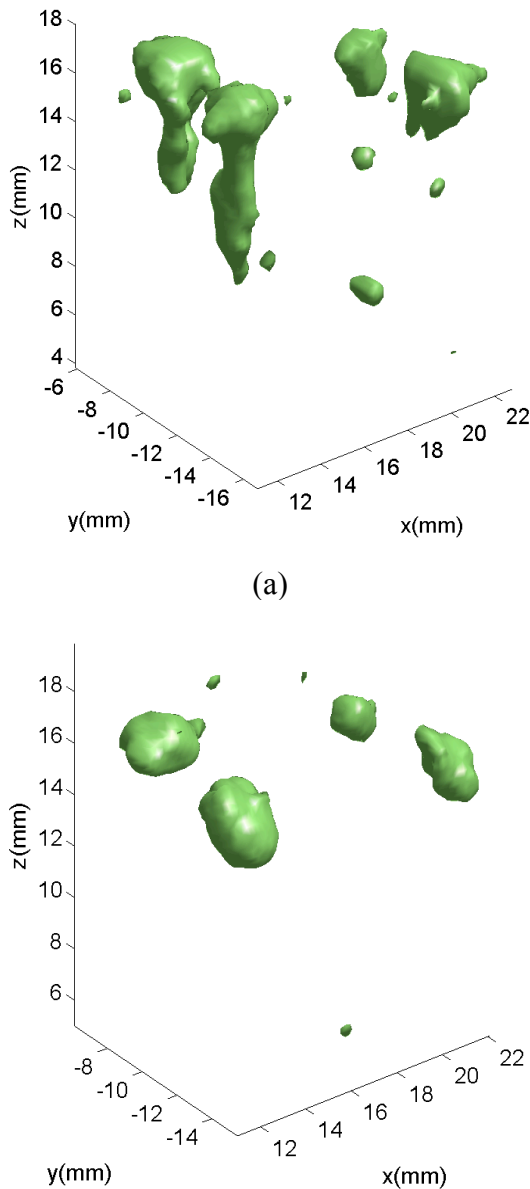


Figure 6(a) Seed isosurfaces calculated at 0.3 μm RMS vibration amplitude at a beam angle of 0°. Note the ring down artifacts descending from the seeds. The transducer is at the top of the image at a height of 32mm. (b) Vibration isosurfaces formed from multiplication (logical AND) of two segmented volumes acquired 30° apart. The ring down tails are effectively eliminated.

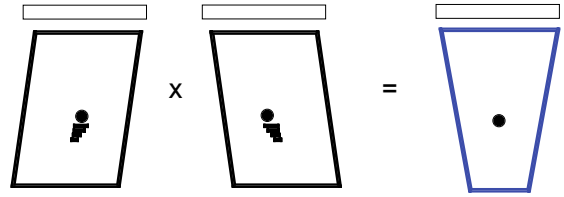


Figure 7. Schematic illustration of compounding method to suppress ring-down tails. Tails appear to radiate in the direction of beam propagation and change direction as beam is steered, while the seed location remains constant regardless of steering angle. Multiplicatively combining multiple look directions eliminates tails and maintains seeds.

IV. CONCLUSION

Finite element calculations of torque on seed cores have been found to be in good agreement with known analytical solutions and allow extension to non-spheroidal geometries. Torque has been found to have substantial sensitivity to the shape of the ferromagnetic core. Further investigation and determination of an optimal core shape appears warranted.

Phase sensitive detection of seed vibration may be useful in segmenting seeds and linking opposing seed ends, overcoming the dark center in side-view seed segmentations due to the dipole nature of the vibration field. Ring down artifacts are common in images of brachytherapy seeds and may be effectively suppressed in vibration amplitude maps by multiplicative combination of multiple seed look angles.

ACKNOWLEDGMENT

This work was supported by the Congressionally Directed Medical Research Program (CDMRP) Grant W81XWH-04-1-0034, administered by the US Army Medical Research and Materiel Command (USAMRMC). Siemens Medical Solutions USA, Ultrasound Group provided in-kind assistance.

REFERENCES

- [1] S.A. McAleavey, M. Palmeri, S. Gracewski, G.E. Trahey, "Ferromagnetic Brachytherapy seed motion in soft tissue: Models, measurements and ultrasound detection," *Proceedings of the IEEE Ultrasonics Symposium*, pp. 1575-1579, 2002
- [2] S.A. McAleavey, D.J. Rubens, K.J. Parker, "Doppler ultrasound imaging of magnetically vibrated brachytherapy seeds," *IEEE Transactions on Biomedical Engineering*, v 50, n 2, Feb 1, 2003, p 252-255
- [3] T. B. Jones, *Electromechanics of Particles*, Cambridge, 1995
- [4] *Electromagnetics Module User's Guide*, Comsol AB, 2004
- [5] R.K. Wangsness, *Electromagnetic Fields*, John Wiley and Sons, 1986
- [6] J.A. Jensen, *Estimation of Blood Velocities Using Ultrasound*, Cambridge,